Sculptures in S^3

Saul Schleimer
Mathematics Institute
University of Warwick
Coventry CV4 7AL
United Kingdom
s.schleimer@warwick.ac.uk

Henry Segerman*
Department of Mathematics and Statistics
University of Melbourne
Parkville VIC 3010
Australia
segerman@unimelb.edu.au

Abstract

We construct a number of sculptures, each based on a geometric design native to the three-dimensional sphere. Using stereographic projection we transfer the design from the three-sphere to ordinary Euclidean space. All of the sculptures are then fabricated by the 3D printing service Shapeways.

1 Introduction

The three-sphere, denoted S^3, is a three-dimensional analog of the ordinary two-dimensional sphere, S^2. In general, the n–dimensional sphere is a subset of Euclidean space, $\mathbb{R}^{n+1}$, as follows:

$$S^n = \{(x_0, x_1, \ldots, x_n) \in \mathbb{R}^{n+1} \mid x_0^2 + x_1^2 + \cdots + x_n^2 = 1\}.$$

Thus S^2 can be seen as the usual unit sphere in $\mathbb{R}^3$. Visualising objects in dimensions higher than three is non-trivial. However for S^3 we can use stereographic projection to reduce the dimension from four to three. Let $N = (0, \ldots, 0, 1)$ be the north pole of S^n. We define **stereographic projection** $\rho : S^n - \{N\} \to \mathbb{R}^n$ by

$$\rho(x_0, x_1, \ldots, x_n) = \left(\frac{x_0}{1 - x_n}, \frac{x_1}{1 - x_n}, \ldots, \frac{x_{n-1}}{1 - x_n} \right).$$

See [1, page 27]. Figure 1a displays stereographic projection in dimension one. For any point $(x, y) \in S^1 - \{N\}$ draw the straight line L through N and (x, y). Then L meets $\mathbb{R}^1$ at a single point; this is $\rho(x, y)$. Notice that the figure is also a two-dimensional cross-section of stereographic projection in any dimension. Additionally, there is nothing special about the choice of $N = (0, \ldots, 0, 1)$. We may alter the formula so that any point in S^3 becomes the **projection point**.

By adding in a point at infinity corresponding to the north pole, stereographic projection extends to a homeomorphism from S^n to $\mathbb{R}^n \cup \{\infty\}$. So we may use stereographic projection to represent, in $\mathbb{R}^3$, objects that live in S^3.

2 The geometry of S^3

A generic plane in $\mathbb{R}^4$, meeting S^3, meets S^3 in a circle. The following **circline property** is fundamental: stereographic projection maps any circle $C \subset S^3$ to a circle or line in $\mathbb{R}^3$. Accordingly we use the word **circline** as a shorthand for circles and lines in $\mathbb{R}^3$. See [1, Section 3.2] for a more general discussion. Note that a circle C of S^3 maps to a line in $\mathbb{R}^3$ if and only if C meets the projection point.

*This work is in the public domain.

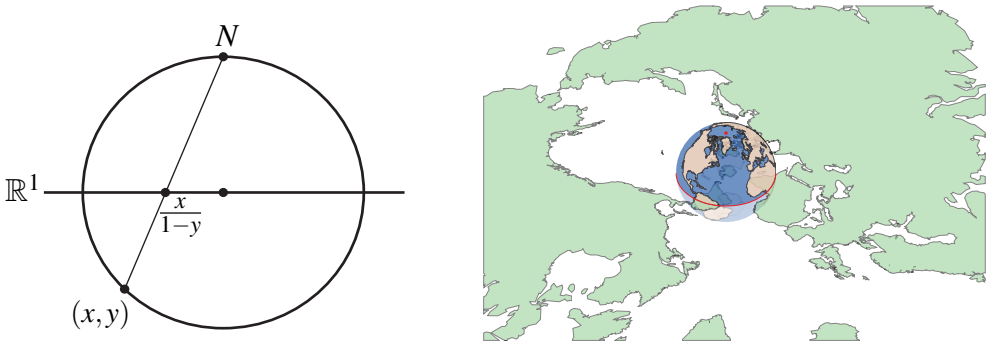

(a) Stereographic projection from $S^1 - \{N\}$ to $\mathbb{R}^1$.

(b) Two-dimensional stereographic projection applied to the Earth. Notice that features near the north pole are very large in the image.

Figure 1: Stereographic projection.

Any plane, meeting the origin in $\mathbb{R}^4$, cuts S^3 in a **great circle**. The great circles are the geodesics, or locally shortest paths, in the geometry on S^3. Just as for the usual sphere, S^2, two distinct great circles meet at two points: say at $x \in \mathbb{R}^4$ and also at the antipodal point $-x$.

Stereographic projection is **conformal**: if two circles in S^3 intersect at a given angle then the corresponding circlines in $\mathbb{R}^3$ meet at the same angle. So stereographic projection preserves angles [1, Section 3.2]. Note that lengths are not preserved; as shown in Figure 1b the distortion of length becomes infinite as we approach the projection point. However, this defect is unavoidable; there is no isometric embedding of any open subset of the three-sphere into $\mathbb{R}^3$.

The quaternionic picture of S^3 In order to get a sense of the shape of S^3, it is useful to have some landmarks. A good way to do this is to view S^3 in terms of the unit quaternions [2]. The quaternions are an extension of the complex numbers, from two dimensions to four. A quaternion is a formal sum $a+bi+cj+dk$ where $a,b,c,d \in \mathbb{R}$ and where i,j,k are non-commuting symbols satisfying

$$i^2 = j^2 = k^2 = ijk = -1.$$

The set of quaternions is called $\mathbb{H}$ in honour of Hamilton, its discoverer. There is a natural bijection between $\mathbb{R}^4$ and $\mathbb{H}$ via $(a,b,c,d) \mapsto a+bi+cj+dk$. So we may view S^3 as the set of **unit quaternions**: those with length $|a+bi+cj+dk| = \sqrt{a^2+b^2+c^2+d^2}$ equal to one. Once this is established the points $\pm 1, \pm i, \pm j, \pm k$ serve as our landmarks. See Figure 2. All of the circlines shown correspond to great circles in S^3 with particularly nice quaternionic expressions.

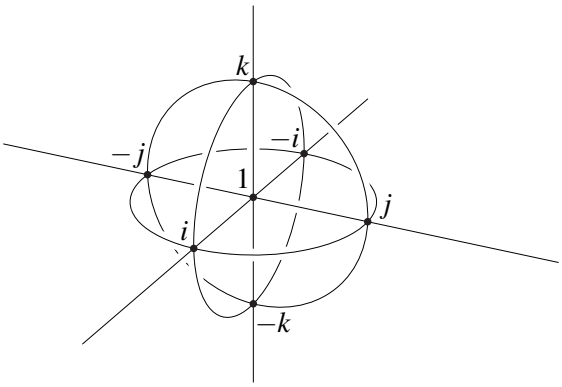

Figure 2: The unit quaternions in S^3 stereographically projected to $\mathbb{R}^3$ from the projection point -1.

The isometries of S^3 The isometries of S^1 are the rigid motions of $\mathbb{R}^2$ that fix the origin, namely rotations and reflections. Under composition, these form the **orthogonal group** $O(2)$. Analogously, the isometries of S^n form the group $O(n)$. The unit quaternions can be realised as a subgroup of $O(4)$ in the following manner. As above we identify $\mathbb{H}$ and $\mathbb{R}^4$. For $q \in \mathbb{H}$ with $|q| = 1$, the map $f_q : \mathbb{H} \to \mathbb{H}$ given by $f_q(x) = q \cdot x$ is an

element of $O(4)$. So, if we want to move the point a to the point b in S^3, then one way to achieve this is to apply the isometry corresponding to the quaternion $b \cdot a^{-1}$.

An application of this technique is to adjust the stereographic projection of a subset of S^3. If $F \subset S^3$ is a surface then, as q varies, the image of $q \cdot F$ in $\mathbb{R}^3$ changes dramatically. Equivalently we can think of this as moving the projection point.

3 Designs in S^3

3.1 Four-dimensional polytopes

Suppose that $\sigma \subset \mathbb{R}^n$ is a finite set. Then $P = P(\sigma)$, the convex hull of σ, is a **polytope** [11, page 4]. Suppose that $\tau \subset \sigma$. If $P(\tau)$ lies in the boundary of P and if for all $\tau \subsetneq \mu \subset \sigma$ we have $\dim P(\tau) < \dim P(\mu)$ then we say $P(\tau)$ is a **face** of P. Let $P^{(k)}$ be the k**–skeleton**: the union of the k–dimensional faces of P. A maximal chain of faces

$$P(\tau_0) \subset P(\tau_1) \subset \ldots \subset P(\tau_n) = P$$

is called a **flag**. Then P is **regular** if for any two flags F and G of P there is an isometry of $\mathbb{R}^n$ that preserves P and sends F to G.

In dimensions one, two, and three the regular polytopes are known of old. These are the interval, the regular k–gons, and the **Platonic solids**: the tetrahedron (simplex), the cube, the octahedron (cross-polytope), the dodecahedron, and the icosahedron. In all higher dimensions there are versions of the simplex, cube, and cross-polytope. In dimension four these are known as the 5–cell, the 8–cell, and the 16–cell. Surprisingly, the only remaining regular polytopes appear in dimension four! There are only three of them: the 24–cell, the 120–cell, and the 600–cell [3, page 136].

Suppose P is a regular n–polytope. The extreme symmetry of P implies that we can move P so that the vertices $P^{(0)}$ lie in the unit sphere, S^{n-1}. Projecting radially from the origin transfers the one-skeleton $P^{(1)}$ from $\mathbb{R}^n$ into S^{n-1}. Stereographic projection then places $P^{(1)}$ in $\mathbb{R}^{n-1}$.

Applied to a 4–polytope, these projections turn the Euclidean geometry of $P^{(1)}$ first into a design of arcs of great circles in S^3 and then into a design of segments of circlines in $\mathbb{R}^3$. If $P^{(1)}$ meets the projection point then the design includes line segments running off to infinity. Coincidentally, Figure 2 shows this for the 16–cell. In order to produce such a design as a physical object, we need to thicken the circline segments to have non-zero volume. One possible approach uses the Euclidean geometry of $\mathbb{R}^3$: we could thicken all segments of the design to get tubular neighbourhoods of constant radius. However, the result is not satisfactory; near the origin in $\mathbb{R}^3$ the tubes are much too thick compared to their separation.

A better solution is to use tubular neighbourhoods in the intermediate S^3 geometry. For this we must parameterise the image of such a tube under stereographic projection. Here the circline property is very useful. The boundary of a tubular neighbourhood of a geodesic in S^3 can be made as a union of small circles in $\mathbb{R}^4$. (These circles lie in S^3, but are not great.) The small circles map to circlines in $\mathbb{R}^3$, which can be directly parameterised. Computer visualisation of stereographic projections of 4-polytopes, in this style, are beautifully rendered by the program Jenn3d [8]. In Figure 3 we show four views of a 3D print of the 24–cell, with the projection point chosen to be at the center of one of the cells. See also Ocneanu's "Octacube" [9].

The sculpture in Figure 3 illustrates a problem inherent in 3D printing of stereographic projections. Suppose that P is a symmetric design in S^3 and $Q = \rho(P)$ is the stereographic projection from the north pole, N. In this case the largest features of Q will correspond to the parts of P closest to N. These are the main contributers to volume and thus to cost. The smallest features of Q will be roughly half the size of the parts of P nearest the south pole. The 3D printing process places a lower bound on the size of the smallest printable feature: current technology allows around 1 mm.

Of course we may scale Q in $\mathbb{R}^3$; scaling up ensures printability while scaling down reduces volume. Thus printability and cost are in tension. For example, if we rotate the 120–cell so that N lies at the center of

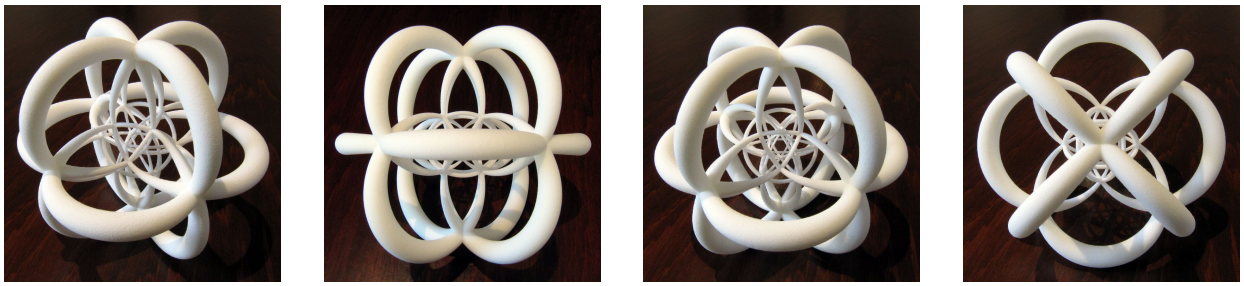

(a) A generic viewpoint. (b) A 2-fold symmetry axis. (c) A 3-fold symmetry axis. (d) A 4-fold symmetry axis.

Figure 3: 24–Cell, 2011, $9.0 \times 9.0 \times 9.0$ cm.

a dodecahedral face, and stereographically project, then the largest feature is around 29.4 times larger than the smallest. So here scaling to ensure printability also ensures unaffordability.

One solution to this problem, as employed by Hart [5], is use a **projective transformation** instead of stereographic projection. This takes a 4–polytope to its **Schlegel diagram** [11, page 133]. This is typically much more compact. However, conformality is lost; the resulting figure distorts both lengths and angles.

Our alternative, shown in Figure 4, is to only print half of the object. We cut S^3 along the equatorial S^2; the sphere equidistant from the north and south poles. Choosing the north pole as the projection point, we project the half of the design in the southern hyperhemisphere. The image is contained in the unit ball $\mathbb{B}^3 = \{x \in \mathbb{R}^3 : |x| \leq 1\}$. This done, the thinnest and thickest parts differ only by a factor of two, at the most. For stereographic projection, parts of the design near the projection point are the real problem, in terms of size. Eliminating the half nearest the projection point eliminates the problem.

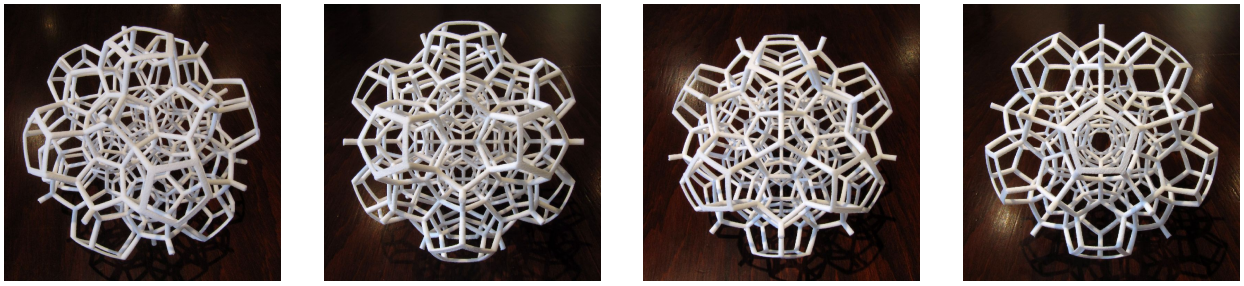

(a) A generic viewpoint. (b) A 2-fold symmetry axis. (c) A 3-fold symmetry axis. (d) A 5-fold symmetry axis.

Figure 4: Half of a 120-Cell, 2011, $9.9 \times 9.9 \times 9.9$ cm.

Note that half of the 120–cell is still very complicated! However, one can understand the whole of the 120–cell by imagining reflecting the object across the cutting two-sphere. Note as well, that printing only the southern half of a design allows us to print objects that pass through the north pole, which ordinarily would be infinitely expensive. For example, in Figure 5 we show one-half of the stereographic projection of the vertex centered 600–cell. This version of the 600–cell is positioned so as to be dual to the facet-centered 120-cell shown in Figure 4. The other half of the vertex-centered 600–cell cannot be printed because the vertex antipodal to the origin meets the projection point.

3.2 Parameterisations of surfaces and torus knots

The geometry of S^3 lends itself particularly well to the representation of tori and torus knots. There seem to be two reasons for this. First, in its natural position certain geodesics in the torus are great circles in S^3. Second, quaternionic multiplication and its relatives directly parametrise torus knots.

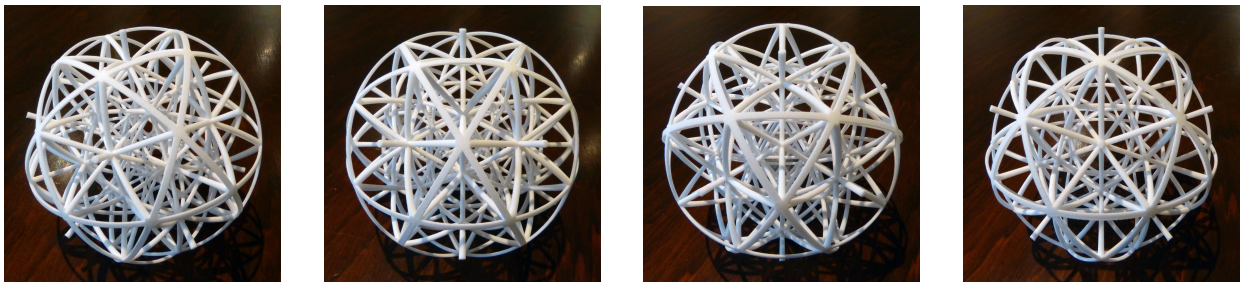

(a) A generic viewpoint. (b) A 2-fold symmetry axis. (c) A 3-fold symmetry axis. (d) A 5-fold symmetry axis.

Figure 5: Half of a 600-Cell, 2011, $9.9 \times 9.9 \times 9.9$ cm.

When representing a surface as a 3D printed object, it is often a good idea to drill holes in the surface, both to save on material used and so the viewer can see, partly, through the surface to what is behind. In our approach, the pattern of holes shows the parameterisation, by realising the surface as a grid with grid-lines in the direction of the parameters.

Clifford torus Recall that $e^{i\theta} = \cos(\theta) + i\sin(\theta)$ parametrises a great circle S^1. The same formula holds replacing i everywhere by j or by k. A Clifford torus is foremost a torus, and so can be parameterised as a product [4, page 139] via

$$\begin{aligned}\mathbb{T} = S^1 \times S^1 &= \left\{ \frac{1}{\sqrt{2}}\big(\cos(\alpha), \sin(\alpha), \cos(\beta), \sin(\beta)\big) \;\middle|\; 0 \le \alpha < 2\pi, 0 \le \beta < 2\pi \right\} \\ &= \left\{ \frac{1}{\sqrt{2}}\big(e^{i\alpha} + e^{i\beta} \cdot j\big) \;\middle|\; 0 \le \alpha < 2\pi, 0 \le \beta < 2\pi \right\}.\end{aligned}$$

The factor of $1/\sqrt{2}$ rescales the torus to lie inside of the unit sphere $S^3 \subset \mathbb{R}^4$. Note that if we vary α while fixing β, then the point traces out a $(1,0)$ curve on $\mathbb{T}$. Conversely varying β while fixing α yields a $(0,1)$ curve. Unfortunately none of these curves are great circles in S^3.

On the other hand, if we vary α and β simultaneously, at the same (respectively, opposite) velocity the the point traces out a $(1,1)$ (respectively $(1,-1)$) curve. As we shall see, these are great circles.

Note that $\mathbb{T}$ divides S^3 into a pair of isometric **solid tori**: copies of $S^1 \times D^2$. We want to rotate the torus $\mathbb{T}$ so that it meets the projection point. This way, after stereographic projection there is a pleasing symmetry; the two solid tori are interchangeable by an isometry of $\mathbb{R}^3$.

We can use quaternions to fix the parameterisation, giving us the desired $(1,1)$ and $(1,-1)$ curves, and to also move $\mathbb{T}$ to meet the projection point $1 \in S^3 \subset \mathbb{H}$. Solving the second problem first, note that $\frac{1}{\sqrt{2}}(1+j)$ lies in $\mathbb{T}$. If q is the quaternion satisfying $\frac{1}{\sqrt{2}}(1+j)q = 1$, then $q = \frac{1}{\sqrt{2}}(1-j)$. The new parameterisation of the torus is given by post-multiplication by q:

$$\frac{1}{\sqrt{2}}\big(e^{i\alpha} + e^{i\beta} \cdot j\big) \cdot \frac{1}{\sqrt{2}}(1-j) = \frac{1}{2}\big(e^{i\alpha} + e^{i\beta} + (e^{i\beta} - e^{i\alpha}) \cdot j\big).$$

The torus meets the desired projection point when $\alpha = \beta = 0$.

We now solve the second problem, by rotating the coordinates through 45°. Take new coordinates θ, ϕ where $\theta = (\alpha+\beta)/2$ and $\phi = (\alpha-\beta)/2$. So $\alpha = \theta + \phi$ and $\beta = \theta - \phi$. Plugging in and simplifying, the above parametrisation becomes $e^{i\theta}e^{-k\phi}$. Keeping ϕ fixed and varying θ now gives a $(1,1)$ curve, which is also a great circle. Note that we only need $0 \le \theta < 2\pi, 0 \le \phi < \pi$ to cover the whole torus. We permute coordinates and change a sign to get a slightly neater form:

$$e^{i\phi}e^{j\theta} = \big(\cos(\theta)\cos(\phi), \cos(\theta)\sin(\phi), \sin(\theta)\cos(\phi), \sin(\theta)\sin(\phi)\big)$$

for $0 \leq \theta < 2\pi, 0 \leq \phi < \pi$. The operations of permuting the coordinates and changing the sign are symmetries of S^3, so the geometry is unchanged and the surface $\mathbb{T}$ still meets the desired projection point, 1. The resulting parametrization is Lawson's minimal surface $\tau_{1,1}$; see [6].

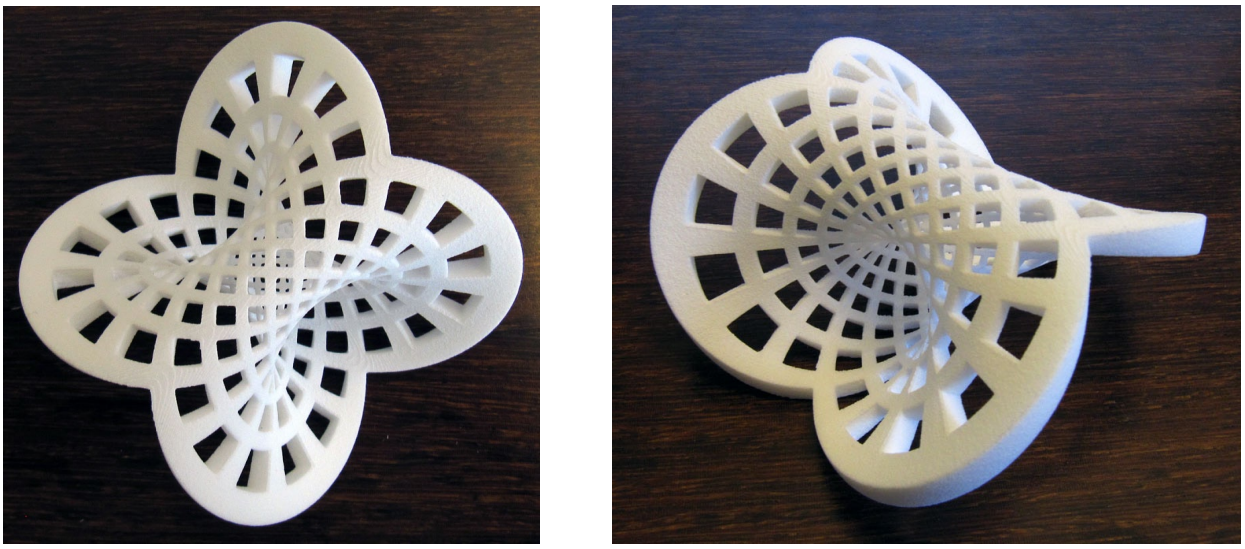

(a) A 2-fold symmetry axis.

(b) A generic viewpoint.

Figure 6: Clifford Torus, 2011, $10.8 \times 10.8 \times 3.4$ cm.

Finding the normal After stereographic projection, we get a 2-dimensional surface in $\mathbb{R}^3 \cup \{\infty\}$. As in Section 3.1, for 3D printing we must thicken our design to have positive volume. Our plan is to additionally parametrise the **normal** (that is, perpendicular) to the surface, and then thicken in that direction. As before, we do this thickening in S^3 rather than $\mathbb{R}^3$.

Suppose that F is any surface in S^3, with parametrisation $p(\theta,\phi) \in S^3 \subset \mathbb{R}^4$. Compute the tangent vectors $\frac{\partial}{\partial\theta}p(\theta,\phi)$ and $\frac{\partial}{\partial\phi}p(\theta,\phi)$ in $\mathbb{R}^4$. Since F lies in S^3, these vectors are tangent to S^3 and so perpendicular to $p(\theta,\phi)$, thought of as a vector from the origin. The desired normal vector $n(\theta,\phi)$ is a unit vector that is perpendicular to the three given vectors p, $\frac{\partial}{\partial\theta}p$, and $\frac{\partial}{\partial\phi}p$. This determines n up to sign. Thus finding n amounts to computing the kernel of the matrix with rows p, $\frac{\partial}{\partial\theta}p$ and $\frac{\partial}{\partial\phi}p$. As these vectors vary with the parameters θ and ϕ it is most convenient to compute n via an application of Cramer's rule: n is the determinant of the matrix with first three rows p, $\frac{\partial}{\partial\theta}p$, $\frac{\partial}{\partial\phi}p$, and fourth row the vector $(1,i,j,k)$.

For the above parametrisation of the Clifford torus we find:

$$\begin{array}{rcl}
p(\theta,\phi) & = & \big(\cos(\theta)\cos(\phi), \quad \cos(\theta)\sin(\phi), \quad \sin(\theta)\cos(\phi), \quad \sin(\theta)\sin(\phi) \big) \\
\frac{\partial}{\partial\theta}p(\theta,\phi) & = & \big(-\sin(\theta)\cos(\phi), \quad -\sin(\theta)\sin(\phi), \quad \cos(\theta)\cos(\phi), \quad \cos(\theta)\sin(\phi) \big) \\
\frac{\partial}{\partial\phi}p(\theta,\phi) & = & \big(-\cos(\theta)\sin(\phi), \quad \cos(\theta)\cos(\phi), \quad -\sin(\theta)\sin(\phi), \quad \sin(\theta)\cos(\phi) \big) \\
n(\theta,\phi) & = & \big(-\sin(\theta)\sin(\phi), \quad \sin(\theta)\cos(\phi), \quad \cos(\theta)\sin(\phi), \quad -\cos(\theta)\cos(\phi) \big)
\end{array}$$

We introduce the parameter ψ for the thickness of the surface. We move a distance ψ along the geodesic from $p(\theta,\phi)$ to $n(\theta,\phi)$ to reach $r(\theta,\phi,\psi) = \cos(\psi)p(\theta,\phi) + \sin(\psi)n(\theta,\phi)$. Let $N_\varepsilon(\mathbb{T})$ be the ε–neighborhood of $\mathbb{T}$, taken in S^3. This is the same as thickening $\mathbb{T}$ in the normal direction, using r.

Since $N_\varepsilon(\mathbb{T})$ contains the projection point, the sculpture $\rho(N_\varepsilon(\mathbb{T}))$ would have infinite volume. We therefore remove a rectangular solid from $N_\varepsilon(\mathbb{T})$; the boundary of the removed material is visible around the outside of the sculpture shown in Figure 6.

(a) A 2-fold symmetry axis. (b) A generic viewpoint.

Figure 7: Round Möbius Strip, 2011, $15.2 \times 10.9 \times 6.2$ cm.

(a) The 4-fold symmetry axis. (b) One of the 2-fold symmetry axes. (c) The other 2-fold symmetry axis.

Figure 8: Round Klein Bottle, 2011, $15.2 \times 15.2 \times 10.9$ cm.

Möbius strip and Klein Bottle A slight variant of the torus gives a Möbius strip:

$$\left\{\left(\cos(\theta)\cos(\phi), \cos(\theta)\sin(\phi), \sin(\theta)\cos(2\phi), \sin(\theta)\sin(2\phi)\right) \mid 0 \le \theta < \pi, 0 \le \phi < \pi\right\}$$

This is a parameterisation of the "Sudanese Möbius strip" [7]. The border of the Möbius strip is given by the points for which θ is 0 or π. Since these points form a geodesic in S^3, the boundary is a circline in $\mathbb{R}^3$ by the circline property. With the given parameterisation, stereographic projection from $(0,0,-1,0)$ gives a circular boundary as in Figure 7. The normal vector is calculated analogously to the torus case, as follows.

$$\begin{aligned}
p(\theta,\phi) &= \left(\cos(\theta)\cos(\phi), \cos(\theta)\sin(\phi), \sin(\theta)\cos(2\phi), \sin(\theta)\sin(2\phi) \right) \\
\tfrac{\partial}{\partial\theta} p(\theta,\phi) &= \left(-\sin(\theta)\cos(\phi), -\sin(\theta)\sin(\phi), \cos(\theta)\cos(2\phi), \cos(\theta)\sin(2\phi) \right) \\
\tfrac{\partial}{\partial\phi} p(\theta,\phi) &= \left(-\cos(\theta)\sin(\phi), \cos(\theta)\cos(\phi), -2\sin(\theta)\sin(2\phi), 2\sin(\theta)\cos(2\phi) \right) \\
n(\theta,\phi) &= \tfrac{1}{\sqrt{1+3\sin^2(\theta)}} \left(-2\sin(\theta)\sin(\phi), 2\sin(\theta)\cos(\phi), \cos(\theta)\sin(2\phi), -\cos(\theta)\cos(2\phi) \right)
\end{aligned}$$

Again the surface is punctured at the projection point, with a rectangular hole in the grid pattern. See Perry's sculpture "Zero" [10] for a similar design. If we extend the strip across its boundary, taking $0 \le \theta < 2\pi$, we get the union of two punctured Möbius strips, giving the twice-punctured Klein bottle shown in Figure 8. This parameterisation of the (unpunctured) Klein bottle is Lawson's surface $\tau_{2,1}$.

Torus knot A further variant gives a parameterisation of a torus knot, in this case the trefoil knot:

$$\left\{\left(\cos(\theta)\cos(\phi), \cos(\theta)\sin(\phi), \sin(\theta)\cos((3/2)\phi), \sin(\theta)\sin((3/2)\phi)\right) \mid 0 \le \phi < 4\pi\right\}$$

Here θ has a fixed value, greater than 0 and smaller than $\pi/2$. Altering the fraction $3/2$ will produce other torus knots. The normal vector may be found as before; however for this model we used an "alternative" to the normal vector, namely

$$n(\theta,\phi) = \big(-\sin(\theta)\sin(\phi), \sin(\theta)\cos(\phi), \cos(\theta)\sin((3/2)\phi), -\cos(\theta)\cos((3/2)\phi)\big).$$

Using the local coordinates (θ,ϕ,ψ), we can add small features to the sculpture, using any shape we could define in ordinary 3-dimensional space. In the case shown in Figure 9, we add cog teeth, which are simply truncated pyramids in (θ,ϕ,ψ) coordinates. The alternative normal vector adds a slight shear slope to the teeth, which we feel is aesthetically preferable.

Figure 9: Knotted Cog, 2011, $3.8 \times 3.4 \times 1.3$ cm.

4 Future directions

Our sculptures are tangible representives of topological and geometric abstractions. In order to do this, we naturally must construct designs that occur in $\mathbb{R}^3$: that is, in actual space. In each case we attempted to choose the most canonical such geometries available and then the most faithful projections.

There is a wild array of further topological and combinatorial objects. For example, there is a rich theory of knots and surfaces and their interrelations. We have not yet found (or perhaps better, understood) satisfactory geometric representations, or at least representatives which map to $\mathbb{R}^3$ in satisfactory ways. An example of the latter problem would be surfaces of genus at least two. These have nice hyperbolic structures, but they cannot be mapped into $\mathbb{R}^3$ in a very satisfying way.

References

[1] Alan F. Beardon, *The geometry of discrete groups*, Graduate Texts in Mathematics, vol. 91, Springer-Verlag, New York, 1983.

[2] John H. Conway and Derek A. Smith, *On quaternions and octonions: their geometry, arithmetic, and symmetry*, A K Peters Ltd., Natick, MA, 2003.

[3] H. S. M. Coxeter, *Regular polytopes*, third ed., Dover Publications Inc., New York, 1973.

[4] Manfredo Perdigão do Carmo, *Riemannian geometry*, Mathematics: Theory & Applications, Birkhäuser Boston Inc., Boston, MA, 1992, Translated from the second Portuguese edition by Francis Flaherty.

[5] George W. Hart, *4d polytope projection models by 3d printing*, to appear in Hyperspace.

[6] H. Blaine Lawson, *Complete minimal surfaces in S^3*, Annals of Mathematics **92** (1970), no. 3, 335–374.

[7] D. Lerner and D. Asimov, *The Sudanese Möbius band (video)*, In SIGGRAPH Video Review, 1984.

[8] Fritz H. Obermeyer, *Jenn3d*, a computer program for visualizing Coxeter polytopes, available from http://www.math.cmu.edu/f̃ho/jenn/.

[9] Adrian Ocneanu, *Octacube*, http://science.psu.edu/news-and-events/2005-news/math10-2005.htm.

[10] Charles Perry, *Zero*, http://www.charlesperry.com/sculpture/zero.

[11] Günter M. Ziegler, *Lectures on polytopes*, Graduate Texts in Mathematics, vol. 152, Springer-Verlag, New York, 1995.